Removal of barium and strontium from wastewater and radioactive wastes using a green bioadsorbent, *Salvadora persica* (Miswak)

Saad S.M. Hassan[a], Ayman H. Kamel[a], Maha A. Youssef[b], Awaad H.A. Aboterika[c], Nasser S. Awwad[d,*]

[a]Department of Chemistry, Faculty of Science, Ain Shams University, Cairo, Egypt, emails: saadsmhassan@yahoo.com (S.S.M. Hassan), ahkamel76@sci.asu.edu.eg (A.H. Kamel)
[b]Analytical Chemistry and Control Department, Hot Laboratories Center, Atomic Energy Authority of Egypt, P.O. 13759 Abu Zaabal, Cairo, Egypt, email: maha_hasa@yahoo.com (M.A. Youssef)
[c]Central laboratory, Faculty of Science, Ain Shams University, Cairo, Egypt, email: awaad_2000@hotmail.com (A.H.A. Aboterika)
[d]Department of Chemistry, Faculty of Science, King Khalid University, P.O. Box: 9004, Abha, Saudi Arabia, Tel. +966549323204; email: aawwad@kku.edu.sa (N.S. Awwad)

ABSTRACT

The adsorption ability of *Salvadora persica* (Miswak) root powder was tested as a green biosorbent for the removal of barium and strontium from wastewater and radioactive wastes. The structure of the powder SP(M) and its chemical properties were characterized and evaluated by Fourier transform infrared spectrometry and scanning electron microscope morphology. The adsorption efficiency has been investigated as a function of pH, contact time, adsorbent dose, and initial metal ions concentration. The experimental data were analyzed using equilibrium isotherm, and kinetic models. The isotherm data agreed fairly well with Langmuir and Freundlich isotherm models. According to the Langmuir isotherm model, the maximum adsorption capacity was sufficiently high compared with many of the previously reported adsorbents and found to be 34.97 and 41.49 mg/g for Ba(II) and Sr(II), respectively. Miswak proved to be suitable and efficient biosorbent, environmentally friendly, cost-effective, and obtained from naturally and widely grown trees in many parts of the world.

Keywords: Removal of barium and strontium; Adsorption; *Salvadora persica* (Miswak); Radioactive waste; Wastewater.

1. Introduction

Radioactive waste resulting from many applications of radionuclides in industry, agriculture, medicine, research, and nuclear reactors has a negative impact on human health and the environment [1]. Barium and strontium ions are the most toxic radionuclides present in relatively large amounts in radioactive liquid wastes arising from the reprocessing plants [2]. Both ions are bone-seeking elements and have carcinogenic effects. Barium compounds dissolve easily in water, thus they have a great potential to spread over long distances. The aquatic organisms tend to accumulate barium compounds in their bodies over time, which can cause undesired effects [3]. Strontium is absorbed by the human body and tends to accumulate in the liver, lungs, and kidneys. Excessive amounts may cause oxygen shortage, anemia, and in the worst case, cancer, because of the damage to the genetic material in body cells [4]. Strontium-90 (^{90}Sr) has been considered as one of the highly-concerned radioactive hazards since the Fukushima nuclear event in 2011 [5–7]. Due to its chemical similarity to calcium

---

* Corresponding author.

and ease of mobility, ^{90}Sr causes a great threat to human beings and other life-forms [8]. Many barium compounds are released during some industrial processes, readily dissolve in water, and are found in lakes, rivers, and streams. Because of their water-solubility, barium compounds can spread over great distances. When fish and other aquatic organisms absorb barium compounds, barium will accumulate in their bodies [9]. On the other hand, barium forms insoluble salts with other common species in the environment, such as carbonate and sulfate, and thus decrease its mobility and poses little risk. Barium compounds that are persistent in the environment usually remain in soil surfaces, or in the sediment of water soils [10]. Small amounts of water-soluble barium compounds may cause some diseases such as breathing difficulties, increased blood pressures, heart rhythm changes, etc. [10,11]. Consequently, effective and simple methods are needed for the removal of these compounds before disposing of their wastes in an aquatic system [2].

Various methods and techniques have been developed for the removal of Sr(II) and Ba(II) from aqueous solutions, including chemical precipitation [12], adsorption [13], ion exchange [14] and separation by membranes [15]. Adsorption has been established as an effective and economical technology to concentrate and remove contaminants from aqueous phases and soils. In this e process, contaminants are separated from the aqueous phase and immobilized in a suitable adsorbent from which they can safely be disposed of or recovered [16,17]. Varieties of adsorbents including pecan shell-based activated carbon, alginate microsphere, natural clays, inorganic-organic hybrid composites, porous silica, and polymers have been suggested for the removal of Sr(II) and Ba(II) in aqueous solutions [18–23].

Salvadora persica (SP(M), Arak, *Galenia asiatica*, Meswak, Mis-wak, Peelu, Pilu, is a popular teeth cleaning stick commonly used in Arab and Muslim countries. The fresh leaves of the plant are eaten as part of a green salad and utilized in traditional medicine [24]. The wood of the *Salvadora persica* is used for charcoal and firewood, the mustard bush is used as drought-resistant fodder for cattle and the seeds are used to extract a detergent oil [25,26].

The organic part of SP(M) sticks of consists mainly of cellulose, hemicelluloses, and lignin. The lignin content in the pulp is higher than its content in the outer layers [27]. The inorganic part provides strong evidence that the mineralogy of the content depends on the geography of the sample's regions [27]. SP(M) was used for the removal of some organic dyes [28,29] and heavy metals (e.g., lead, cadmium, copper, and nickel) [30].

The present study describes the removal of Ba(II) and Sr(II) from aqueous media and [133]Ba and ^{90}Sr radioactive radionuclides from radioactive waste solutions using SP(M) powder as a green bioadsorbent, under batch conditions. The adsorption equilibrium data for the binary component system were analyzed using Langmuir and Freundlich isotherms. The separation method was also extended to remove [133]Ba and ^{90}Sr radioactive radionuclides from radioactive wastes. A comparison with data obtained with some previously used adsorbents revealed a significant efficiency of SP(M) for the removal of barium and strontium compounds from wastewater and radioactive waste.

2. Experimental

2.1. Materials

All the chemicals used were of analytical grade and were obtained from Sigma-Aldrich located at St. Louis, MO, USA. Synthetic stock solution of $Sr(NO_3)_2$ and $Ba(NO_3)_2$ were prepared in deionized water (Millipore Super Q system with resistivity of 18.2 MΩ) located at Akishima, Japan. Nitric acid and sodium hydroxide solutions were used to adjust the solution to the desired pH. The raw SP(M) was obtained from Mekka, Saudi Arabia. The sticks of SP(M) were washed with deionized water, dried at 105°C for 24 h., and blended in a blender. The SP(M) powder was sieved to obtain adsorbent with particle size between 90 and 250 μm. All solutions resulted from the equilibrium experiment studies, were filtered off through a 0.45 μm membrane filter and the filtrate was analyzed.

2.2. Instrumentation

Thermo Scientific/Dionex ICS-1100 ion chromatography (IC) system was used for Ba(II) and Sr(II) determination. An Orion digital pH/mV meter (model SA 720) in conjunction with a combination glass electrode (Orion 81-02) was used for all pH measurements. Fourier transform infrared (FTIR) spectrometry was carried out with a Thermo-Nicolet model iS10. The surface micro-morphology of materials was investigated using a Jeol-JSM-1200EX II scanning electron microscope (SEM). The gamma-ray of [133]Ba has been measured radiometrically by high resolution (7.5%) NaI(Tl) detector model 802–3X3, Canberra, USA, and the beta ray of ^{90}Sr was measured using liquid scintillation analyzer TRI–CARB model (2700TR series).

2.3. Adsorption kinetic study

2.3.1. Effect of contact time

Aliquots (20.0 mL) of 25 mg/L Ba(II) and Sr(II) ion solutions were added to conical flasks containing 0.15 g of SP(M). The mixtures were agitated at a speed of 150 rpm at 25°C for different time periods (15, 30, 60, 90, 120, and 150 min). The SP(M) was separated by filtration, and Ba(II) and Sr(II) contents in the filtrate were determined using IC. The percentage removal (*R*, %) was calculated according to the following equation:

$$R = \frac{C_0 - C_e}{C_0} \times 100 \qquad (1)$$

where R is the percent removal of Ba(II) and Sr(II), C_0 and C_e are the initial Ba(II) and Sr(II) concentrations and C_e is the final equilibrium Ba(II) and Sr(II) concentrations (mg/L).

2.3.2. Effect of sorbent dosage

Portions of SP(M) ranging from 0.05 to 0.25 g were transferred to different 25 mL flasks. Aliquots of 20.0 mL Ba(II) and Sr(II) solution (25.0 mg/L) were added. The flasks were capped and placed in a shaking bed for continuous equilibration for 1 h. The contents of each flask were filtered

off using a 0.45 μm filtration membrane and the filtrate was subjected to IC or radiometric analysis.

2.3.3. Effect of solution pH

Solutions containing 20.0 mL of 25 mg/L of Ba(II) and Sr(II) were prepared and transferred to the flasks. Concentrated HNO₃ and NaOH solutions were used to adjust the initial pHs from 3.0 to 10.0 followed by the addition of 0.15 g portions of SP(M) and the mixtures were left to equilibrate for 1 h at 25°C.

2.3.4. Effect of initial metal concentration

Three 20.0 mL aliquots of Ba(II) and Sr(II) solutions with initial concentrations at 10, 15.0, 20, and 25.0 mg/L were separately mixed with 0.15 g SP(M) powder in conical flasks at 25°C. The mixtures were allowed to equilibrate, filtered through a 0.45 μm filtration membrane and their metal contents were measured by IC.

2.4. Adsorption isotherms study

Adsorption isotherms were obtained with different initial concentrations of Ba(II) and Sr(II) while maintaining SP(M) dosage at a constant level. In order to correct for any adsorption of Ba(II) and Sr(II) on the container surface, control experiments were carried out in the absence of SP(M). These experiments indicated that no adsorption by the container walls was detected. In all experiments, the difference between the initial Ba(II) and Sr(II) concentrations (C_0) and the equilibrium concentrations (C_e) was calculated and used to determine the adsorptive capacity (q_e) as follows:

$$q_e = \frac{V}{m}(C_0 - C_e)\,\mathrm{mg\,/\,g} \tag{2}$$

where V, is the total volume of tested solution (L), m is the mass of adsorbent used (g); C_0, is the initial concentration of the Ba(II) and Sr(II) solution (mg/L); and C_e, is the residual Ba(II) and Sr(II) concentrations (mg/L).

The linear model, which describes the accumulation of solute by sorbent as directly proportional to the solution concentration is presented by the relation:

$$q_e = K_D C_e \tag{3}$$

The constant of proportionality or distribution coefficient K_D is often referred to as the partition coefficient.

The Langmuir model represents one of the first theoretical treatments of non-linear sorption and has been successfully applied to a wide range of systems that exhibit limiting or maximum sorption capacities. The model assumes uniform energies of adsorption onto the surface and no transmigration of the adsorbate in the plane of the surface.

The Langmuir isotherm is given by:

$$q_e = \frac{Q^o b C_e}{1 + b C_e} \tag{4}$$

where Q^o and b are Langmuir constants related to adsorption capacity and energy of adsorption, respectively [31,32]. Eq. (4) is usually linearized by inversion to obtain the following form:

$$\frac{1}{q_e} = \frac{1}{Q^o} + \frac{1}{bQ^o}\frac{1}{C_e} \tag{5}$$

Eq. (5) is equally used to analyze batch equilibrium data by plotting $1/q_e$ vs. $1/C_e$, which yields a linear plot if the data conform to the Langmuir isotherm. The essential characteristics of Langmuir isotherm can also be expressed in terms of a dimensionless constant separation factor or equilibrium parameter (R_L), which is defined by Eq. (6) [33].

$$R_L = \frac{1}{1 + bC_0} \tag{6}$$

where C_0 is the initial solute concentration and b is Langmuir's adsorption constant (L/mg). The R_L value confirms the adsorption to be unfavorable ($R_L > 1$), linear ($R_L = 1$), favorable ($0 < R_L < 1$) or irreversible ($R_L = 0$) [34].

Freundlich isotherm is the most widely used non-linear sorption model and is given by the general form:

$$q_e = K_F C_e^n \tag{7}$$

where K_F relates to sorption capacity and n to sorption intensity. The logarithmic form of Eq. (7) given below is usually used to fit data from batch equilibrium studies:

$$\log q_e = \log K_F + \frac{1}{n}\log C_e \tag{8}$$

3. Results and discussion

3.1. Influence of adsorbent dose

The removal percentages of Ba(II) and Sr(II) by SP(M) were studied at adsorbent doses of 0.05, 0.1, 0.15, 0.20, and 0.25 g. Initial metal concentration and temperature were maintained at 25 mg/L and 25°C. The results of the dependence of Ba(II) and Sr(II) sorption on the amount of SP(M) dose are shown in Fig. 1. It can be seen that, an increase in the sorbent concentration causes an increase in the Ba(II) and Sr(II) adsorption. In general, the number of sites available for adsorption increases with the increase in adsorbent dosage and reaches a maximum at the highest adsorbent dose. Also, the available sites for the adsorption increase with the increase of the adsorbent dosage [35], probably because a fixed adsorbent dose can only adsorb a certain amount of adsorbate. Therefore, the more the adsorbent dosage, the larger the quantity of adsorbate that can be adsorbed [36].

3.2. Influence of contact time

The adsorption of Ba(II) and Sr(II) on SP(M) was studied as a function of shaking (contact) time ranging from

30–150 min, whereas other parameters were kept constant. The removal percent of Ba(II) and Sr(II) by SP(M) increases with the increase of shaking time (Fig. 2). At the start, the ions adsorbed and occupied selectively the active sites on the SP(M). As the contact time increased the active sites on the adsorbents become saturated and the rate of adsorption gradually decreases to reach a plateau.

3.3. Influence of pH

It is well documented that the adsorption process is influenced by the pH of the test solution, which affects the surface charge of the adsorbent and the degree of ionization of adsorbate. Fig. 3 shows the effect of pH on the adsorption efficiency of SP(M) towards Ba(II) and Sr(II) ions. A sharp increase of Ba(II) and Sr(II) adsorption was observed between pH 3.5 and 6, then it slightly increased above pH 7. This behavior is due to the zero net surface charge of the adsorbent (pHpzc) which was found to be around pH 6. At a pH above 7, the surface of the SP(M) becomes negatively charged, which enhances the adsorption of positively charged Ba(II) and Sr(II) ions through the electrostatic force of attraction. At pH value lower than 6, the surface of the adsorbent becomes positively charged, inhibiting the adsorption of Ba(II) and Sr(II) ions due to the electrostatic repulsion between the adsorbent and adsorbate. Furthermore, at low pH levels, H^+ ions compete with Ba(II) and Sr(II) cations for the same adsorption site. In addition, the solution pH could greatly affect the activity of adsorbent functional groups. The dissociation of the acidic functional groups of the adsorbent is minimal at lower pH values and hinders binding of the Ba(II) and Sr(II) ions.

3.4. Effect of Ba(II) and Sr(II) concentrations

The effect of initial Ba(II) and Sr(II) concentrations on the adsorption capacity of SP(M) was studied in the range of 10–25 mg metal/L. The temperature was maintained at 25°C and an adsorbent dose of 0.15 g/L were used (Fig. 4). The amount of Ba(II) and Sr(II) adsorbed on the SP(M) increased with the increase of initial concentration of Ba(II) and Sr(II) until reaching the equilibrium state, where the adsorbent active sites become saturated.

3.5. Adsorption isotherm

Adsorption isotherms are essential tools to investigate the nature of the adsorption process and play a vital role
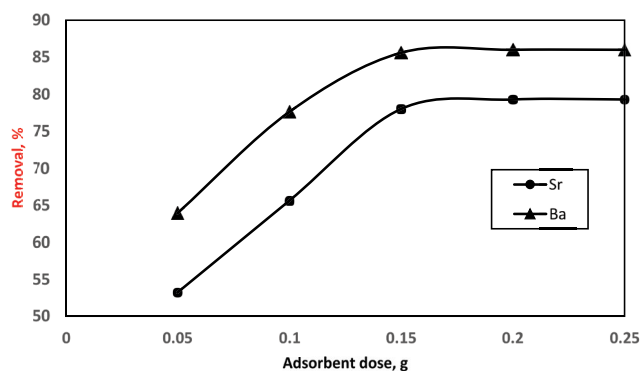
Fig. 1. Effect of adsorbent dosage on the removal of Ba(II) and Sr(II) by SP(M). Conditions: C_0, 25 mg/L; time of contact, 60 min; pH, 7; and temperature, 25°C.
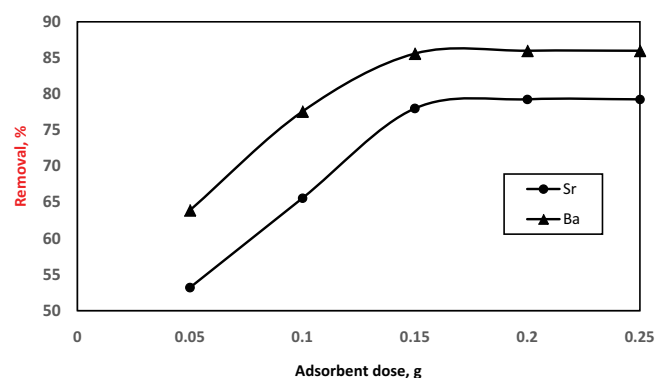
Fig. 2. Effect of contact time on the removal of Ba(II) and Sr(II) by SP(M). Conditions: C_0, 25 mg/L; adsorbent dose, 0.15 g; pH, 7; and temperature, 25°C.
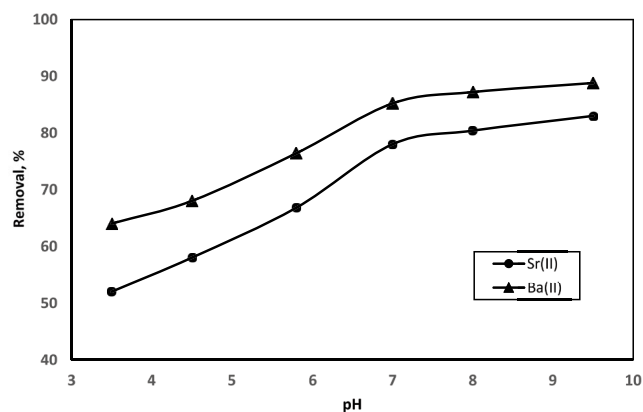
Fig. 3. Effect of pH on the removal of Ba(II) and Sr(II) by SP(M). Conditions: C_0, 25 mg/L; adsorbent dose, 0.15 g; and temperature, 25°C.
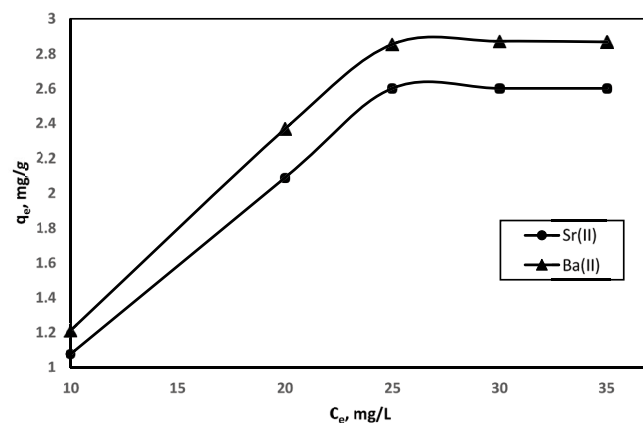
Fig. 4. Effect of initial metal concentration on adsorption of Ba(II) and Sr(II) onto SP(M).

in the determination of the maximum adsorption capacity. Adsorption isotherms also used to estimate the economic viability of an adsorbent for commercial success. Various adsorption isotherms such as Langmuir and Freundlich models [37,38] were studied in this work to determine the adsorption capacity of the SP(M).

3.5.1. Ba(II) adsorption isotherms

Langmuir model assumes that maximum adsorption corresponds to a saturated monolayer of adsorbate molecules on the adsorbent surface. A linear plot (Fig. 5) of specific adsorption $(1/q_e)$ against the equilibrium concentration $(1/C_e)$ with the correlation coefficient of 0.9997 (Table 1). The calculated Langmuir monolayer adsorption capacity was found to be 34.97 mg/g. The value of dimensionless separation factor $(R_L = 0.909)$, is between 0 and 1, indicating that adsorption of Ba(II) onto SP(M) is a favorable process (Fig. 5).

The Freundlich model is commonly used to describe heterogeneous systems. The Freundlich parameter $1/n = 0.9437$ obtained from the plot (Fig. 6 and Table 1) falls between 0 and 1 suggesting that the adsorption is linear and uniform throughout the adsorbent surface. Based on the R^2 values obtained from various isotherms studied in this work, the best-fitted adsorption isotherms were in the order of prediction precision: Langmuir > Freundlich isotherms and their corresponding R^2 values are 0.9997 and 0.9993.
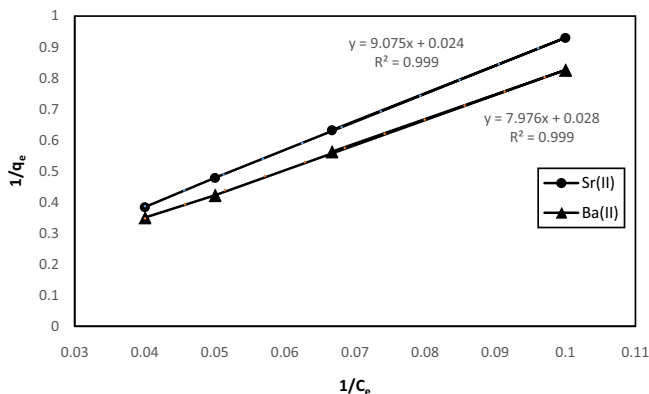
Fig. 5. Langmuir isotherm plot of Ba(II) and Sr(II) adsorption on SP(M).

Table 1
Adsorption isotherm parameters for Ba(II) and Sr(II) adsorption on SP(M)

Model	Parameter	Ba(II)	Sr(II)
Langmuir	Q^o (mg/g)	34.97	41.49
	b (L/mg)	0.0040	0.0027
	R_L	0.9090	0.9377
	R^2	0.9997	0.9999
Freundlich	K [(mg/g)(L/mg)$^{1/n}$]	0.138	0.117
	$1/n$	0.9437	0.9630
	R^2	0.9993	1

3.5.2. Sr(II) adsorption isotherms

Fitting of Sr(II) adsorption data to the Langmuir model (Fig. 5) resulted in a correlation coefficient of 0.9999 (Table 1), indicating the suitability of the model. The monolayer adsorption capacity calculated was 41.49 mg/g. The value of dimensionless separation factor $(R_L = 0.9377)$, is between 0 and 1, which indicates that adsorption of Sr(II) onto SP(M) is favorable.

Freundlich parameter $1/n = 0.9630$ obtained from the plot (Fig. 6 and Table 1) falls between 0 and 1 which suggests that the adsorption is uniform throughout the adsorbent surface. Based on the R^2 values obtained from various isotherms studied in this work, the best-fitted adsorption isotherms were in order: Freundlich > Langmuir isotherms and their corresponding R^2 values are 1 and 0.9999.

3.5.3. Adsorption mechanism

The results obtained indicated that the adsorption of Sr(II) onto SP(M) was higher than Ba(II). The difference in the adsorption capacity is probably due to the adsorption mechanism, and metal selectivity based on ionic radius and electronegativity. The ionic radius influences the adsorption rate of the metal ions. The adsorption capacity for the metal ions increases with decreasing the ionic radii [39]. A higher ionic radius of Ba(II) (1.48 Å) than Sr(II) (1.28 Å) [40] explains the lower adsorption capacity for Ba(II) when compared with Sr(II). Steric and overcrowding at the adsorption sites occur with larger radius barium ion [41]. The diffusion of metal ions with smaller radii (barium) is comparatively faster than the ions with a larger radius (strontium). Similar trends with ions having different ionic radii have been reported [42,43]. The adsorption of metal ions with higher electronegativity is higher than those with lower electronegativity. The electronegativity is Sr(II) (1.0) is greater than Ba(II) (0.9). Thus, adsorption of Sr(II) is higher when compared with Ba(II).

An additional factor that could be considered, is the hydrolysis of metal ions. The hydrolysis equilibrium reaction can be expressed as:

$$M^{2+} + H_2O \rightleftharpoons MOH^+ + H^+ \tag{9}$$

$$MOH^+ + H_2O \rightleftharpoons M(OH)_2 + H^+ \tag{10}$$
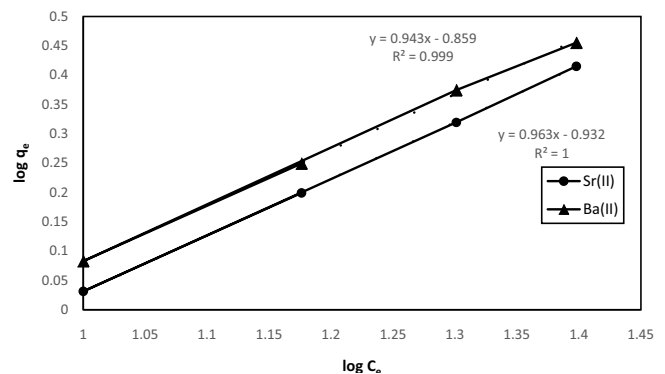
Fig. 6. Freundlich isotherm plot of Ba(II) and Sr(II) adsorption on SP(M).

The hydration enthalpies of the metals, Ba(II) = –1,309 kJ/mol, and Sr(II) = –1,446 kJ/mol, indicate that Ba(II) has a higher tendency to hydrolyze and form hydroxide as compared with Sr(II) [43]. As the adsorption takes place after hydrolysis, the metal ions available for binding with the negatively charged functional groups of the adsorbent are lesser in the case of Ba(II) compared with Sr(II).

The mechanism of removal of Ba(II) and Sr(II) from aqueous solutions by using SP(M) can be explained (Fig. 7) by three sequential steps: (i) migration of both ions from the bulk test solution to the SP(M)'s surface through the liquid film (external diffusion or film diffusion) due to the concentration gradient between the bulk solution and the pore surface, (ii) migration of both ions from the SP(M) surface to the interior part (pores) of the SP(M) to reach the end of the pore (internal diffusion or particle diffusion or intra-particle diffusion) due to the concentration gradient between the pore mouth and pore end, and (iii) finally, attachment of both ions to the end of the pore through the adsorbent –OH and COOH active sites by adsorption and/or ion exchange. Here, the actual physical and/or chemical adsorption occurs, with ion exchange/complexation reactions.

FTIR analysis of SP(M) before and after adsorption of Ba(II) and Sr(II) was also conducted and shown in Fig. 8. FTIR measurement of SP(M) powder showed the presence of the following functional groups: stretching vibration of OH groups (3,400–3,900 cm^{-1}), C–H bonds stretching due to alkynes (2,000–2,400 cm^{-1}), stretching of C=O group due to presence of carboxylic acid, lactone, aldehyde, and ketones (1,700–1,800 cm^{-1}, NH group (1,515 cm^{-1}), C=C stretching of aromatic rings (1,500–1,556 cm^{-1}), and C–O linkage that might be due to ether or phenols (1,000–1,300 cm^{-1}).

The spectrum of SP(M) after separation of Ba(II) and Sr(II), displayed almost the same bands with a noticeable increase in the % transmittance without variation in the locations of the bands. This means an interaction occurs between the adsorbate and the metal ions with a change in dipole moment which causes intensification of the absorption bands.

The surface morphology of SP(M) powder was investigated by SEM at a magnification of 1500. The SEM images of SP(M) are shown in Fig. 9. The microstructure of SP(M) image showed that the surface contains small pores probably used for uptake of Ba(II) and Sr(II). Also, the microstructure of SP(M) showed that the cells are nearly spherical in shape.

3.6. Application of SP(M) for removal of radioactive ^{133}Ba and ^{90}Sr

The adsorption experiment for radioactive ^{133}Ba and ^{90}Sr was carried out by the addition of SP(M) to a solution of the stable Ba(II) and Sr(II) metal ions followed by spiking with ^{133}Ba (3448 Bq/L) or ^{90}Sr (13421 Bq/L) radionuclide. The pH of the solution was adjusted at pH 7, shaken for 1 h at ambient temperature (25°C), centrifuged, filtered off through 0.45 mm filter paper followed by radiometric monitoring of ^{133}Ba and ^{90}Sr ions at intervals of time. Under the same condition the supernatant from the previous step (first cycle) was kept for the second cycle using freshly prepared SP(M). Two cycles were needed for the complete

Fig. 7. Adsorption mechanism for the removal of Ba(II) and Sr(II) from aqueous solution by SP(M).
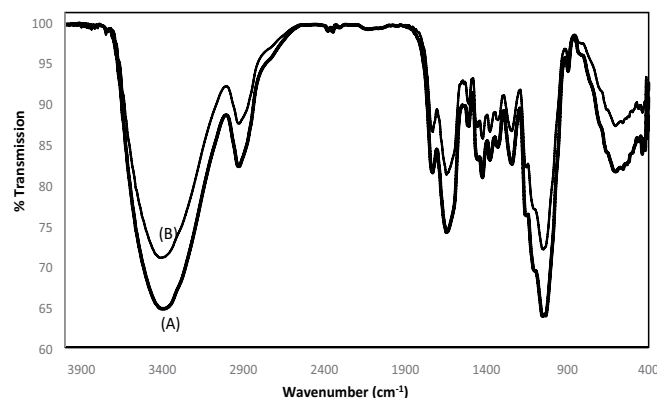
Fig. 8. FTIR spectra of SP(M), (a) before and (b) after contact with Ba(II) and Sr(II) solutions.
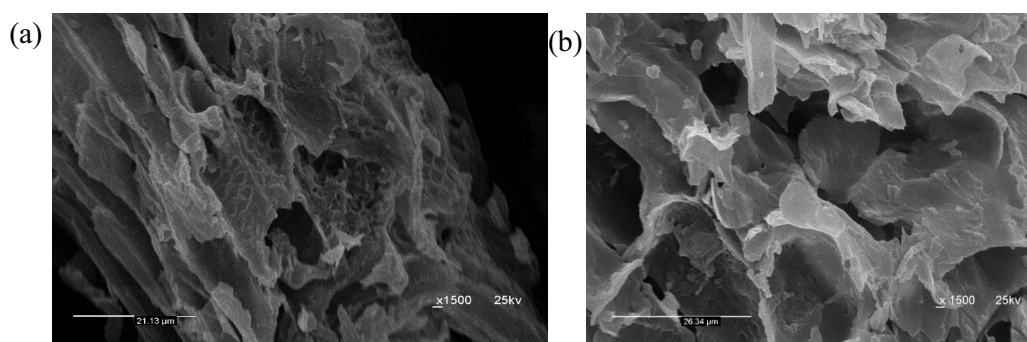
Fig. 9. Scanning electron micrograph (SEM) of SP(M), (a) before and (b) after contact with Ba(II), and Sr(II) solutions.

removal of both radioactive [133]Ba and [90]Sr. This decrease in uptake may be due to the blocking of some active sites on exposure to ionizing radiations [2]. These results clearly reveal that SP(M) has reasonable stability towards radiation damage (Table 2).

3.7. Advantages and comparison with other reported adsorbents

A comparison of the capacity of different previously reported adsorbents with the suggested SP(M) towards the adsorption and removal of Ba(II) and is given in Table 3. Based on the precursor material used, the adsorption capacities vary, mostly because of the differences in the chemical compositions, the method of activation, and the mechanisms of adsorption [44]. It can be seen that the adsorption capacity of SP(M) towards Ba(II) (34.97 mg/g) and Sr(II) (41.49 mg/g) is much better than many of those previously recommended adsorbents. The availability, cost-effectiveness, and performance of SP(M) make it an economically and environmentally friendly potential bioadsorbent for Ba(II), and Sr(II) removal from wastewater and radioactive waste.

4. Conclusions

The present study deals with the use of the root powder of *Salvadora persica* tree, known as Miswak SP(M), for the removal of Ba(II) and Sr(II) from aqueous solutions and radioactive wastes. The major components of SP(M) powder are carboxyl, hydroxyl, and nitrogen-containing, functional groups. The nature of the material allows capturing of Ba(II) and Sr(II) ions efficiently due to the active sites and pore structure. The adsorption performance was strongly affected by some experimental parameters such as pH of the test solution, adsorbent dosage, contact time, and initial Ba(II) and Sr(II) concentrations. The maximum sorption capacity is 34.97 and 41.49 mg/g for Ba(II) and Sr(II) ion, respectively. The results demonstrate that the separation process is due to both ion exchange and adsorption mixed mechanisms. The suggested SP(M) adsorbent powder offers

Table 2
Percentage removal of [133]Ba and ^{90}Sr radionuclide from synthetic radioactive samples by SP(M) sorbent (volume = 15 mL, SP(M) dosage = 0.15 g, conc. = 25 ppm, pH = 7, contact time = 1 h)

	Activity before (Bq/L)	Activity after (Bq/L)	R%
[133]Ba removal			
First cycle	3,448	1,963	43.06
Second cycle	1,963	300	91.3
[90]Sr removal			
First cycle	13,421	8,306	38.1
Second cycle	8,306	2,327	82.66

Table 3
Adsorption capacity of various adsorbents for the adsorption of Ba(II) and Sr(II)

Adsorbent	pH	Contact time, min.	Q_{max} mg/g Ba(II)	Q_{max} mg/g Sr(II)	Ref.
Dolomite powder (anhydrous calcium magnesium carbonate)	5.5	120	3.96	1.17	[3]
Activated sericite (micas, made of muscovite)	7–9	30	–	1.60	[4]
Expanded perlite (natural siliceous volcanic rock)	6.0	90	2.48	1.14	[9]
MXene (two-dimensional inorganic compounds)	6–7	120	9.30	–	[45]
Aerobic granules (biomass)	6.2	120	–	37	[46]
Root tissue powders	6.5	–	–	12.89	[47]
Mn–Zr mixed hydrous oxide	4.1	180	–	30.86	[48]
Activated carbon	4	720	–	44.4	[49]
Pecan shell based activated carbon	6.0	–	3.33	8.80	[50]
NaZTS (Na–Zn–Sn–S quaternary metal sulfide nanosheets)	2–12	5	–	40.4	[51]
Sericite (micas, made of muscovite)	3	60	–	21.41	[52]
Sodium trititanate whisker	5	180	–	8.37	[53]
Synthetic allophane (hydrous aluminum silicate clay mineraloid)	8.5	120	38.6	34.4	[54]
Sea shell *(Donax trunculus)*	6.0	–	–	25.45	[55]
Hydroxyapatite (calcium phosphate mineral)	6–9.4	60	–	2.37	[56]
SP(M) (miswak powder)	7	60	34.97	41.49	This work

significant advantages over many of the previously reported adsorbents. It is cost-effective, green material with high adsorption capacity suitable for fast removal of Ba(II) and Sr(II) ions from wastewater and radioactive wastes.

Acknowledgments

References

[1] M.I. Ojovan, E.L. William, S.N. Kalmykov, Nuclear Waste Regulations, Handbook of an Introduction to Nuclear Waste Immobilisation, 3rd ed., Elsevier, Amsterdm, The Netherlands, 2019, pp. 81–106.

[2] S.P. Mishra, V.K. Singh, Radiotracer technique in adsorption study XIII, adsorption of barium and strontium ions on chromium(IV) oxide powder, Appl. Radiat. Isot., 46 (1995) 847–853.

[3] A. Ghaemi, M. Torab-Mostaedi, M. Ghannadi-Maragheh, Characterizations of strontium(II) and barium(II) adsorption from aqueous solutions using dolomite powder, J. Hazard. Mater., 190 (2011) 916–921.

[4] L. Lalhmunsiama, D. Tiwari, S.M. Lee, Physico-chemical studies in the removal of Sr(II) from aqueous solutions using activated sericite, J. Environ. Radioact., 147 (2015) 76–84.

[5] H. Shimura, K. Itoh, A. Sugiyama, S. Ichijo, M. Ichijo, F. Furuya, Y. Nakamura, K. Kitahara, K. Kobayashi, Y. Yukawa, T. Kobayashi, Absorption of radionuclides from the Fukushima nuclear accident by a novel algal strain, PLoS One, 7 (2012) e44200.

[6] G. Steinhauser, V. Schauer, K. Shozugawa, Concentration of strontium-90 at selected hot spots in Japan, PLoS One, 8 (2013) e57760.

[7] S.Y. Fukuda, K. Iwamoto, M. Atsumi, A. Yokoyama, T. Nakayama, K. Ishida, I. Inouye, Y. Shiraiwa, Global searches for microalgae and aquatic plants that can eliminate radioactive cesium, iodine, and strontium from the radio-polluted aquatic environment: a bioremediation strategy, J. Plant Res., 127 (2014) 79–89.

[8] S. Skupinski, J. Solecki, Studies of strontium(II) sorption on soil samples in the presence of phosphate ions, J. Geochem. Explor., 145 (2014) 124–128.

[9] M. Torab-Mostaedi, A. Ghaemi, H. Ghassabzadeh, M. Ghannadi-Maragheh, Removal of strontium and barium from aqueous solutions by adsorption onto expanded Perlite, Can. J. Chem. Eng., 89 (2011) (1247–1254).

[10] O. Celebi, A. Kilikli, H.N. Erten, Sorption of cesium and barium ions onto solid humic acid, J. Hazard. Mater., 168 (2009) 695–703.

[11] F. Gingele, A. Dahmke, Discrete barite particles, and barium as tracers of paleoproductivity in south Atlantic sediments, Paleoceanogr. Paleoclimatol., 9 (1994) 151–168.

[12] V. Pacary, Y. Barre, E. Plasari, Method for the prediction of nuclear waste solution decontamination by coprecipitation of strontium ions with barium sulfate using the experimental data obtained in non-radioactive environment, Chem. Eng. Res. Des., 88 (2010) 1142–1147.

[13] A. Zhang, C. Chen, E. Kuraoka, M. Kumagai, Impregnation synthesis of a novel macroporous silica-based crown ether polymeric material modified by 1-dodecanol and its adsorption for strontium and some coexistent metals, Sep. Purif. Technol., 62 (2008) 407–414.

[14] A.Y. Zhang, T. Akashi, Electrical conductivity of partially ion-exchanged Sr and Ba β-alumina single crystals determined by a.c. impedance spectroscopy, Mater. Lett., 60 (2006) 2834–2836.

[15] S.V.S. Rao, B. Paul, K.B. Lal, S.V. Narasimhan, J. Ahmed, Effective removal of cesium and strontium from radioactive wastes using chemical treatment followed by ultra-filtration, J. Radioanal. Nucl. Chem., 246 (2000) 413–418.

[16] D. Caputo, F. Pepe, Experiments and data processing of ion exchange equilibria involving Italian natural zeolites: a review, Microporous Mesoporous Mater., 105 (2007) 222–231.

[17] S.S. Gupta, K.G. Bhattacharyya, Immobilization of Pb(II), Cd(II), and Ni(II) ions on kaolinite and montmorillonite surfaces from the aqueous medium, J. Environ. Manage., 87 (2008) 46–58.

[18] A.F. Seliman, Y.F. Lasheen, M.A.E. Youssief, M.M. Abo-Aly, F.A. Shehata, Removal of some radionuclides from contaminated solution using natural clay: bentonite, J. Radioanal. Nucl. Chem., 300 (2014) 969–979.

[19] H. Chen, D. Shao, J. Li, X. Wang, The uptake of radionuclides from aqueous solution by poly(amidoxime) modified reduced graphene oxide, Chem. Eng. J., 254 (2014) 623–634.

[20] H. Faghihian, S.N. Nasrabadi, S. Khonsari, Removal of Sr(II) from aqueous solutions by aminosilane functionalized MCM-48, Sep. Sci. Technol., 49 (2014) 2031–2038.

[21] Y.X. Leng, G. Ye, F.F. Bai, J.C. Wei, J.C. Wang, J. Chen, Synthesis of new periodic mesoporous organosilica (PMO) incorporated with macrocyclic host for strontium binding, Mater. Lett., 110 (2013) 212–214.

[22] Y. Song, Y. Du, D. Lv, G. Ye, J. Wang, Macrocyclic receptors immobilized to monodisperse porous polymer particles by chemical grafting and physical impregnation for strontium capture: a comparative study, J. Hazard. Mater., 274 (2014) 221–228.

[23] G. Ye, F.F. Bai, J.C. Wei, J.C. Wang, J. Chen, Novel polysiloxane resin functionalized with dicyclohexano-18-crown-6 (DCH18C6): synthesis, characterization, and extraction of Sr(II) in high acidity HNO$_3$ medium, J. Hazard. Mater., 225–226 (2012) 8–14.

[24] https://en.wikipedia.org/wiki/Salvadora_persica#cite_note-heritage-3

[25] P.J. Ramoliya, H.M. Patel, A.N. Pandey, Effect of salinization of soil on growth and macro- and micro-nutrient accumulation in seedlings of *Salvadora persica* (*Salvadoraceae*), For. Ecol. Manage., 202 (2004) 181–193.

[26] M.P. Reddy, M.T. Shah, J.S. Patolia, *Salvadora persica*, a potential species for industrial oil production in semiarid saline and alkali soils, Ind. Crops Prod., 28 (2008) 273–278.

[27] F.S. Bahabri, Application of spectroscopic techniques for the identification of organic and inorganic constituents of *Salvadora persica* from Saudi Arabia, Physica A, 276 (2000) 346–351.

[28] T.M. Elmorsi, Equilibrium isotherms and kinetic studies of removal of Methylene blue dye by adsorption onto Miswak leaves as a natural adsorbent, J. Environ. Prot., 2 (2011) 817–827.

[29] E. Bazrafshan, F.K. Mostafapour, M.A. Zazouli, Methylene blue (cationic dye) adsorption into *Salvadora persica* stems ash, Afr. J. Biotechnol., 11 (2012) 16661–16668.

[30] O. Heri, S. Cay, A. Uyanik, N. Erduran, Removal of common heavy metals from aqueous solutions by waste *Salvadora persica* L. branches (Miswak), Int. J. Environ. Res., 8 (2014) 987–996.

[31] I. Langmuir, The adsorption of gases on plane surfaces of glass, mica and platinum, J. Am. Chem. Soc., 40 (1918) 1361–1403.

[32] S. Sarkar, S. Sarkar, P. Biswas, Effective utilization of iron ore slime, a mining waste as adsorbent for removal of Pb(II) and Hg(II), J. Environ. Chem. Eng., 5 (2017) 38–44.

[33] F. Zare, M. Ghaedi, A. Daneshfar, S. Agarwal, I. Tyagi, T.A. Saleh, V.K. Gupta, Efficient removal of radioactive uranium from solvent phase using AgOH–MWCNTs nanoparticles: kinetic and thermodynamic study, Chem. Eng. J., 273 (2015) 296–306.

[34] A.S. Alzaydien, Adsorption of Methylene blue from aqueous solution onto a low-cost natural Jordanian Tripoli, Am. J. Environ. Sci., 5 (2009) 197–208.

[35] P. Maneechakr, S. Karnjanakom, Adsorption behavior of Fe(II) and Cr(VI) on activated carbon: surface chemistry, isotherm, kinetic and thermodynamic studies, J. Chem. Thermodyn., 106 (2017) 104–112.

[36] P.S. Kumar, S. Ramalingam, C. Senthamarai, M. Niranjanaa, P. Vijayalakshmi, S. Sivanesan, Adsorption of dye from aqueous solution by cashew nut shell: studies on equilibrium isotherm, kinetics, and thermodynamics of interactions, Desalination, 261 (2010) 52–60.

[37] S.S.M. Hassan, N.S. Awwad, A.H.A. Aboterika, Removal of chromium(VI) from wastewater using Sorel's cement, J. Radioanal. Nucl. Chem., 269 (2006) 135–140.

[38] S.S.M. Hassan, N.S. Awwad, A.H.A. Aboterika, Removal of mercury(II) from wastewater using camel bone charcoal, J. Hazard. Mater., 154 (2008) 992–997.

[39] L.-C. Lin, M. Thirumavalavan, Y.-T. Wang, J.-F. Lee, Effect of preparation conditions on the adsorption of heavy metal ions from aqueous solution by mesoporous silica materials prepared using an organic template (HDTMAB), J. Chem. Eng. Data, 55 (2010) 3667–3673.

[40] I. Persson, Hydrated metal ions in aqueous solution: how regular are their structures?, Pure Appl. Chem., 82 (2010) 1901–1917.

[41] C. Faur-Brasquet, Z. Reddad, K. Kadirvelu, P. Le Cloirec, Modeling the adsorption of metal ions (Cu^{2+}, Ni^{2+}, Pb^{2+}) onto ACCs using surface complexation models, Appl. Surf. Sci., 196 (2002) 356–365.

[42] J.C. Igwe, A.A. Abia, Adsorption isotherm studies of Cd(II), Pb(II), and Zn(II) ions bioremediation from aqueous solution using unmodified and EDTA modified maize cob, Ecletica Quim., 32 (2007) 33–42.

[43] I. Uzun, F. Güzel, Adsorption of some heavy metal ions from aqueous solution by activated carbon and comparison of percent adsorption results of activated carbon with those of some other adsorbents, Turk. J. Chem., 24 (2000) 291–297.

[44] Y. Zhang, J. Zhao, Z. Jiang, D. Shan, Y. Lu, Biosorption of Fe(II) and Mn(II) ions from aqueous solution by rice husk ash, BioMed Res. Int., 2014 (2014) 1–10.

[45] A.K. Fard, G. McKay, R. Chamoun, T. Rhadfi, H. Preud'Homme, M.A. Atieh, Barium removal from synthetic natural and produced water using MXene as two dimensional (2-D) nano-sheet adsorbent, Chem. Eng. J., 317 (2017) 331–342.

[46] L. Wang, X. Liu, X.-F. Chen, D.-J. Lee, J.-H. Tay, Y. Zhang, C.-I. Wan, Biosorption of Sr(II) from aqueous solutions using aerobic granules: equilibrium and mechanisms, J. Radioanal. Nucl. Chem., 306 (2015) 193–202.

[47] J.P. Chen, Batch and continuous adsorption of strontium by plant root tissues, Bioresour. Technol., 60 (1997) 185–189.

[48] S. Inan, Y. Altas, Adsorption of strontium from acidic waste solution by Mn–Zr mixed hydrous oxide prepared by co-precipitation, Sep. Sci. Technol., 45 (2010) 269–276.

[49] S. Chegrouche, A. Mellah, M. Barkat, Removal of strontium from aqueous solutions by adsorption onto activated carbon: kinetic and thermodynamic studies, Desalination, 235 (2009) 306–318.

[50] A.R. Kaveeshwar, P.S. Kumar, E.D. Revellame, D.D. Gang, M.E. Zappi, R. Subramaniam, Adsorption properties and mechanism of barium(II) and strontium(II) removal from fracking wastewater using pecan shell-based activated carbon, J. Cleaner Prod., 20 (2018) 1–13.

[51] M. Zhang, P. Gu, S. Yan, L. Dong, G. Zhang, Na/Zn/Sn/S (NaZTS): quaternary metal sulfide nanosheets for efficient adsorption of radioactive strontium ions, Chem. Eng. J., 379 (2020) 122227.

[52] B. Hu, Q. Hu, D. Xu, C. Chen, Macroscopic and microscopic investigation on adsorption of Sr(II) on sericite, J. Mol. Liq., 225 (2017) 563–568.

[53] Z.L. Zhang, L. Li, Removal of strontium ions from aqueous solution by adsorption onto sodium trititanate whisker, Adv. Mater. Res., 391–392 (2011) 1173–1178.

[54] A. Baldermann, A.C. Grießbacher, C. Baldermann, B. Purg-staller, I. Letofsky-Papst, S. Kaufhold, M. Dietzel, Removal of barium, cobalt, strontium, and zinc from solution by natural and synthetic allophane adsorbents, Geoscience, 8 (2018) 309–328.

[55] A. Bulut, S. Yusan, S. Aytas, S. Sert, The use of seashell (*Donax trunculus*) powder to remove Sr(II) ions from aqueous solutions, Water Sci. Technol., 78 (2018) 827–836.

[56] Y. Nishiyama, T. Hanafusa, J. Yamashita, Y. Yamamoto, T. Ono, Adsorption and removal of strontium in aqueous solution by synthetic hydroxyapatite, J. Radioanal. Nucl. Chem., 307 (2016) 1279–1285.